ES Energy & Environment
DOI: https://dx.doi.org/10.30919/esee946

C: ZnO Composites for Improving Catalytic Activity of ZnO

Prathamesh Kadam,[1,2] Kisan Gadave,[2] Sandesh Jadkar,[1] Vishal Kadam[1] and Chaitali Jagtap[1,*]

Abstract

Nowadays industries are letting out many reactive dyes making them waste and causing many serious environmental and ecological problems. Many researchers are working on the appropriate method to remove pollutants and impurities from different industries. ZnO is considered as important photocatalyst, due to its excellent properties, including non-toxicity, high redox potential, low cost, and environmentally friendly features. Activated carbon, due to its high surface area and pore volume, is considered the most efficient adsorbent in pollutant removal. It is considered an important adsorbent having a unique structure related to its functional properties. Kinetic studies of dye adsorption on activated carbon and its modified forms are widely studied by many researchers. We have synthesized ZnO by reflux method followed by doping various concentrations (2:1), (1:1) and (1:2) of activated carbon into ZnO. The Photocatalytic experiment is performed with Methylene Blue, Eosin-Y Dye, and Rose Bengal dye. The synthesized ZnO powder and ZnO composite with activated carbon are characterized by various characterization techniques such as UV-Visible Spectra, X-Ray diffraction, and Scanning Electron Microscopy. The band calculated was observed for (a), (b), (c) and (d) respectively to be nearly equal to 3.2 eV. Well-distributed activated carbon attached to the surface of ZnO is observed. The composition of zinc (Zn) and oxygen (O) peaks approves the purity of ZnO nanoparticles. Further, Photocatalytic dye degradation of Methylene Blue dye was observed in 14 min.

Keywords: ZnO; Composite; Activated Carbon; Photodegrdation.
Received: 19 August 2023; Revised: 19 August 2023; Accepted: 23 August 2023.
Article type: Research article.

1. Introduction

Nowadays industries are letting out many reactive dyes making them waste and causing many serious environmental and ecological problems. This dye-containing wastewater is very harmful to aquatic life and ecology.[1] Many researchers are working on the appropriate method to remove pollutants and impurities from different industries.[2] There are many physical and chemical methods used to remove dye.[3,4] Contaminants from waste water leads to skin ulcers, many skin diseases, damage to respiratory and digestive systems and other countless side effects.[5] Photocatalytic treatment of organic pollutants requires photo-excitable semiconductor material like ZnO, TiO_2, ZrO_2, WO_3, *etc*.[6] Recently photocatalytic dye degradation is extensively used for the removal of dyes from wastewater by many scientists over the world.[7,8] Semiconductor photocatalysis is a powerful and cutting-edge approach to wastewater remediation, thereby offering the huge possibility of harnessing naturally available sunlight.[9] ZnO has attracted many researchers due to its low cost,[10] high level of photocatalytic activity,[11] non-toxic nature,[12] chemical stability,[13] and optical properties.[14] The increased degradation efficiency of the carbon source was the main contribution for the improved decolorization of the sludge adding with conductive Polyaniline.[15] When illuminated with an appropriate light source, the photocatalyst generates electron/hole pair with free electrons produced in the empty conduction band leaving positive holes in the valence band. These electron/hole pairs are capable of initiating a series of chemical reactions that eventually mineraliz the pollutants.[16] ZnO can be synthesized by various methods such as the hydrothermal method,[17] Sol-Gel,[18] Precipitation method,[19] Pyrol method,[20] Solvothermal method,[21] Spray pyrolysis,[22] Reflux method.[23] ZnO has various applications such as gas sensors,[24] photocatalysis,[25] Biological,[26] Solar cell,[27] and supercapacitors.[28] Activated carbon, due to its high surface area and pore volume, is considered the most efficient adsorbent in pollutant removal. It is considered an important adsorbent having a unique structure related to its functional properties. Kinetic studies of dye adsorption on activated carbon and its modified forms are

[1] *Advanced Physics Laboratory, Department of Physics, Savitribai Phule Pune University, Pune, 411007.*
[2] *Department of Chemistry, Prof. Ramkrishna More Arts, Commerce & Science College, Pradhikaran, Akurdi, Pune – 411044.*
**Email:* chaitali25jagtap@gmail.com (C. Jagtap)

widely studied by many researchers.[29] Activated carbon is considered a potential absorbent dye and demonstrates the high ability to dye molecules adsorption and high ability to dye molecules adsorption by molecular sieve mechanism. Results of these investigations suggested that the high specific surface area and porous structure of AC were effective in photoactivity via increasing adsorption, which is the determining step in the heterogeneous photocatalytic reaction. Therefore, a combination of adsorption and heterogeneous photocatalysis makes photo-oxidation more beneficial for the dye compound removal from wastewater.[30] The first time new ZnO supporting carbon-based catalysts with highly enhanced catalytic properties promoting the green and selective synthesis of quinoline derivatives.[31]

In the present study, we have synthesized ZnO by reflux method followed by various proportion of activated carbon into ZnO. The Photocatalytic experiment is performed with Methylene Blue, Eosin-Y Dye, and Rose Bengal dye. The synthesized ZnO powder and activated carbon composite ZnO powder are characterized by various characterization techniques such as UV-Visible Spectra, X-Ray diffraction, and Scanning Electron Microscopy.

2. Experimental details

2.1 Materials

All chemicals of analytical grade were used without any further refinement. Zinc Chloride (Thomas Baker), Sodium Hydroxide (SRL), Citric Acid Monohydrate (SRL), Eosin- Y (s-d fine), Rose Bengal (Himedia Laboratories), Methylene Blue (High Purity Chemicals), Double Distilled water.

2.2 Synthesis of pure ZnO nanoparticles and activated carbon doped ZnO

A series of Activated Carbon doped samples were prepared by dissolving zinc chloride, in double distilled water with Activated to obtain 2:1, 1:1 and 1:2. Activated carbon on the ZnO surface respectively. Each 0.2 M zinc precursor solution was dissolved in 100 ml double distilled water subjected to magnetic stirring at 70 °C under refluxed chemical method approach for 2 h, 0.2 M citric Acid was added to the above solution to avoid agglomeration. Then, 2 M sodium hydroxide solution was prepared in 200 ml double distilled water and was added dropwise at the rate of 1 drop per sec. to an above-prepared solution. After the complete addition of sodium hydroxide solution, the total solution was magnetically stirred for 2 hours at 80 °C. The prepared solution was cooled overnight and it appeared blackish. The precipitate collected was then centrifuged multiple times at 4000 rpm and dried at 70 °C for 24 hours. The dried powder was then grinded in a mortar and pestle. The grinded powder was annealed at 450 °C for about 4 hrs. Finally, activated carbon composite with ZnO nanoparticles were obtained. Thus, bare ZnO is named as ‘a’, and ZnO with different composition ratio as 2:1, 1:1 and 1:2 of activated carbon named as ‘b’, ‘c’, ‘d’ was synthesized respectively. The four powders are further characterized by various characterizations.

2.3 Characterizations methods

XRD (D/B max-2400, Rigaku, USA) was used to determine the crystalline nature, phase, and average crystallite size of the ZnO nanoparticle. Morphology was studied using Scanning electron microscopy (SEM) (JEOL JSM 6360-A, USA), Optical study was performed using a UV-Vis spectrophotometer (JASCO V-670, Germany). The photocatalytic degradation of MB was performed under OSRAM 300 W Halogen lamp as the source of visible light (emission range ~400–800 nm).

3. Result and discussion

3.1 Structural analysis

Figure 1 shows the XRD spectra of bare ZnO doped with various concentrations of Activated carbon in the ratio 1:0, 2:1, 1:1, and 1:2. the standard peaks were obtained for all samples at 2θ values 31.74°, 34.42°, 36.26°, 47.58°, 56.62°, 62.90°, 62.42°, 66.96°, 67.91°, 69.08°, 72.58Å, 76.92Å corresponding to the (100), (002), (101), (102), (110), (103), (200), (112), (201), (004), (202). The obtained reflections in all samples correspond to JCPDS card No. 05-0664 with a wurtzite phase and hexagonal structure.

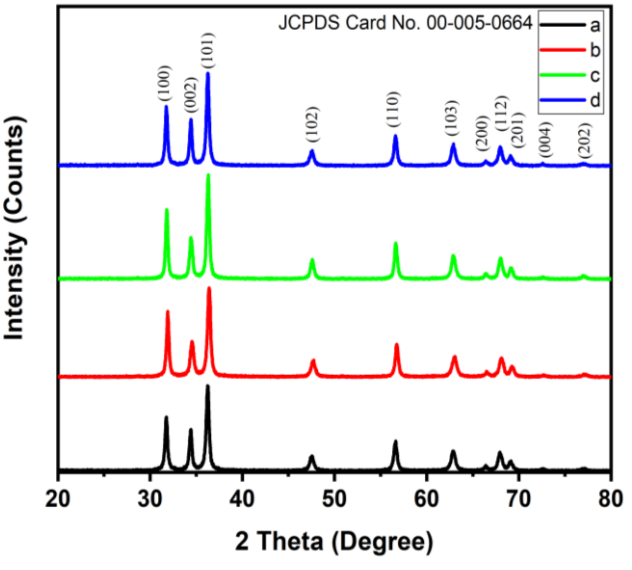

Fig. 1 XRD Pattern of Annealed (a), (b), (c), (d).

3.2 Optical analysis

Figure 2 shows the UV Visible spectra of Activated carbon and ZnO composite with Activated. From the Figure, it is observed that activated carbon completely absorbs the UV-Visible light irradiation.[32,33] The graph is obtained by fitting the Tauc model and Davis -Mott model in the high absorbance as described earlier. The energy band gap is determined by extrapolating the linear line portions to the energy axis.[34,35] The band calculated was observed for ‘a’, ‘b’, ‘c’, and ‘d’ respectively to be nearly equal to 3.2 eV. The lower shift is observed when ZnO is combined with Activated Carbon to form a nanocomposite. Therefore, the visible light absorption

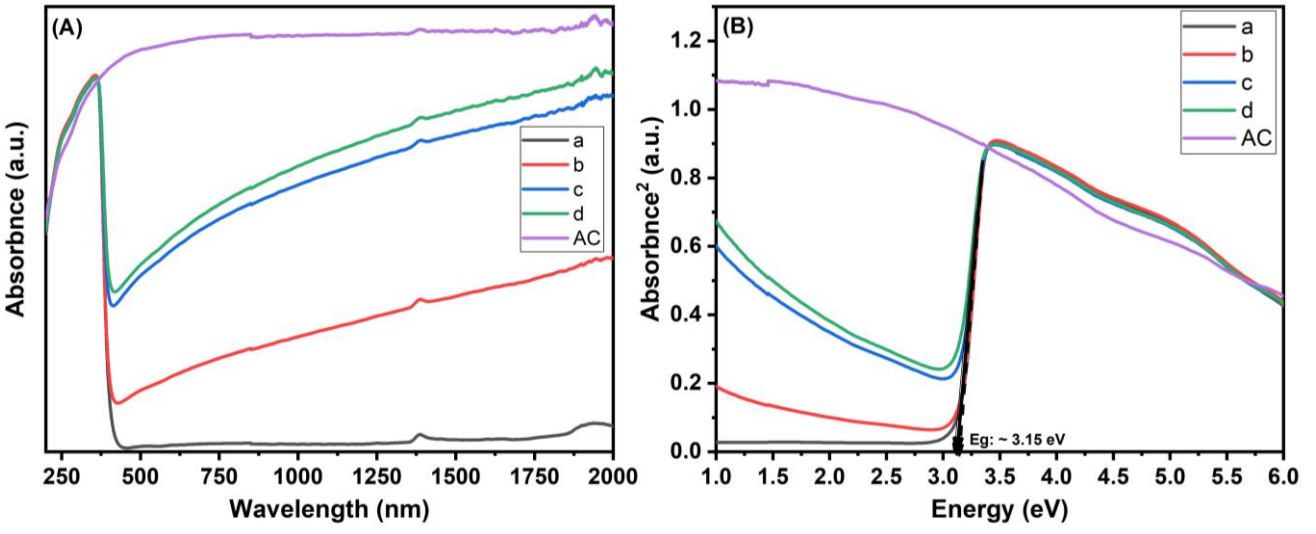

Fig. 2 UV-Visible Spectra of Annealed (a), (b), (c), (d).

of the material increases in carbon content. However activated carbon results in the adsorption of dye but it does not include the degradation of organic compounds, so when a small amount of ZnO is involved, it also helps to degrade organic compounds present in the wastewater. Therefore, Activated Carbon Nanocomposite with ZnO shows better degradation as compared to Only ZnO.

3.3 Morphological analysis

Figure 3 shows well-distributed activated carbon attached to

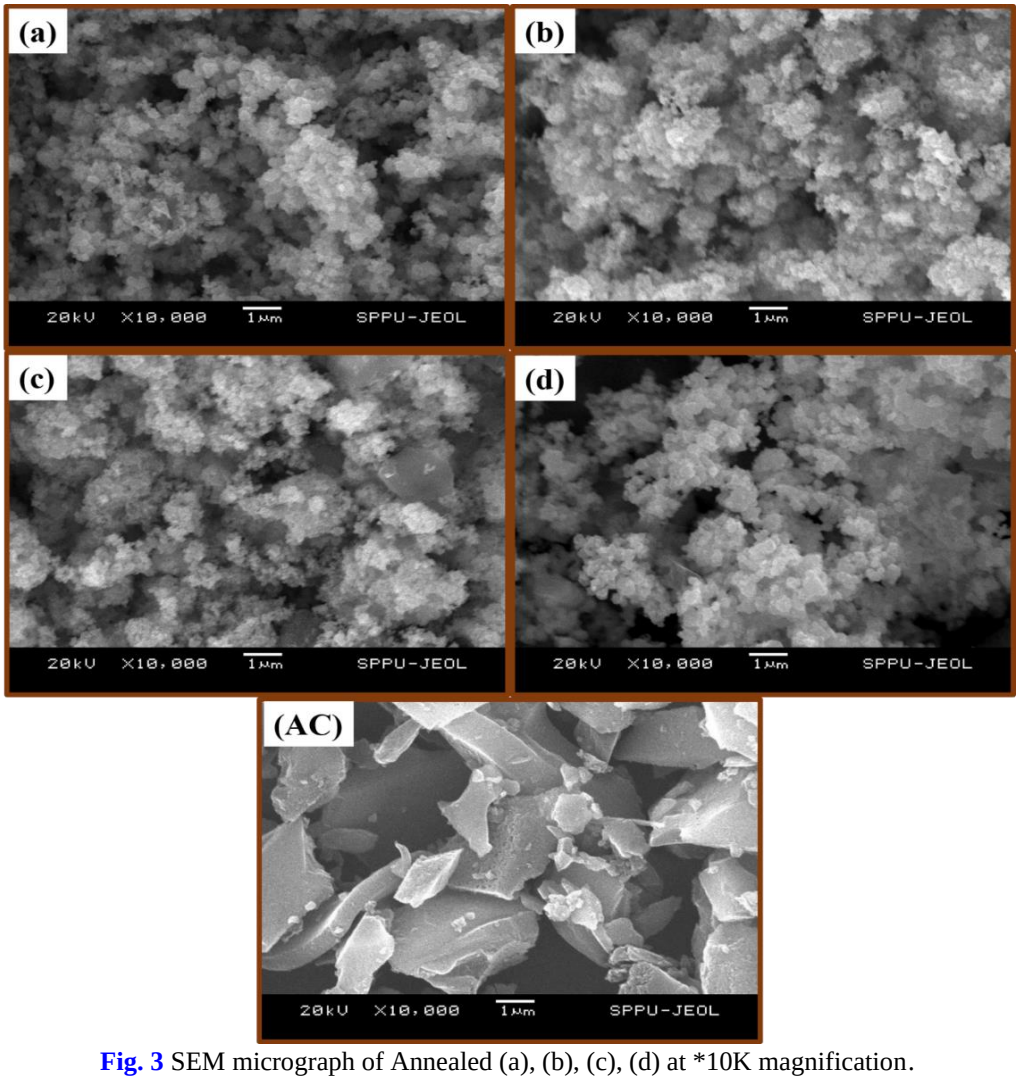

Fig. 3 SEM micrograph of Annealed (a), (b), (c), (d) at *10K magnification.

the surface of ZnO. As the composite ratio changes there is a change in particle size, the decrease in particle size increases the active sites, thereby promoting the adsorption of more organic compounds. The SEM images of activated carbon revealed the microporous and mesoporous morphology. ZnO nanostructures appear as spherical particles that are aggregated to form slightly aggregated nanoparticles. In (b) the nanoparticles are in composite with Activated Carbon. Some traces of activated carbon are observed with ZnO nanoparticles. The particles are observed to be aggregated. In (c) there is an equal amount of activated carbon present, therefore there is equal distribution of ZnO nanoparticles and activated carbon. In (d) the ratio of activated carbon with ZnO is 2:1, therefore, the activated carbon amount is more than ZnO and therefore there is a large amount of activated carbon present in it. In (AC) the SEM image of Activated Carbon is observed to be a flakes-like structure. Diacon *et. al* observed a flake-like structure for activated carbon.[36] Emil observed a flower-like structure for ZnO nanoparticles.[37] Yadav *et. al* reported ZnO -activated nanocomposite in 1:1 ratio nanocomposite with agglomerated particles containing neck with neighbors further forming spindle-like shapes.[38]

3.4 Compositional analysis

Figure 4 shows the Compositional analysis of Annealed of 'a', 'b', 'c', and 'd' The composition of zinc (Zn) and oxygen (O) peaks approve the purity of ZnO nanoparticles. The existence of an Activated carbon array contributes to the composite of AC in the ZnO matrix. Table 1 shows the Atomic Weight percent in ZnO composite with Activated Carbon.

Table 1. Compositional Analysis of Annealed of (a), (b), (c), (d).

Sample	(a)	(b)	(c)	(d)
Element	Atomic wt %			
Zn	51.6	24.3	15.2	6.4
O	48.4	46.5	34.1	28.1
AC	-	29.2	50.7	65.5
Total	100.0	100.0	100.0	100.0

3.5 Photodegradation study

Here, in this study, we have done the photodegradation effect of ZnO and ZnO composite with activated carbon on methylene blue dye. Here we have used 10 ppm dye and 50 mg of powder of ZnO and ZnO/AC. Fig. 5 shows the photodegradation of Methylene Blue dye of 'a', 'b', 'c', and 'd' Bare ZnO, *i.e.* (a) degrades in 100 min, ZnO /AC (2:1), *i.e.* (b) degrades in 100 mi as the active sites available not much as compared to bare ZnO. In (c) the concentration of Activated carbon is equal to the ZnO, therefore, dye degrades in 35 min. In (d) the Activated carbon concentration is twice the bare ZnO which degrades in 14 min. Table 2 shows a literature survey of Dye degradation.

Table 2. ZnO and various composite materials exhibiting degradation time.

Sr. No.	Semiconducting Material	Composite	Dye	Degradation Time	Ref.
1.	TiO_2	Fe_3O_4@Ag@TiO_2	Methylene Blue	120 min	[39]
2.	TiO_2	Ni/NiO/TiO_2	Methylene Blue	120 min	[40]
3.	TiO_2	Porous TiO_2 Ceramic/Ag-Agcl	rhodamine B	50 min	[41]
4.	TiO_2	Mesocrystalline TiO_2/sepiolite	Methylene Blue	160 min	[42]
5.	TiO_2	TiO_2-PDMS	rhodamine B	60 min	[43]
6.	TiO_2	g-C_3N_4 loading on TiO_2/Bentonite	RBR-X3BS	100 min	[44]
7.	ZnO	g- C_3N_4	rhodamine B	120 min	[45]
8.	ZnO	Graphene	Methylene Blue	100 min	[46]
9	ZnO	Biomass	Methylene Blue	120 min	[47]
10.	ZnO	Carbon	Methyl Orange	120 min	[48]
11.	ZnO	Graphitic carbon nitride gCN	Orange II dye	360 min	[49]
12.	ZnO	lignin based	Rhodamine B	50 min	[50]
13.	ZnO	Polyaniline	Acid Blue 25 dye	60 min	[51]
14.	ZnO	$ZnFe_2O_4$	Rhodamine B	180 min	[52]
15.	ZnO	Silver and Graphite	Methylene Blue	20 min	[53]
16.	ZnO	Polyhedral/haemetite/carbon	Rhodamine B	120 min	[54]
17.	ZnO	V_2O_5	Methylene Blue	180 min	[55]
18.	ZnO	Carbon	Rhodamine B	60 min	[56]
19	ZnO	TiO_2/ZnO/Fenton	Methylene Blue	140min	[57]
20.	ZnO	NiO/ZnO	Methylene Blue	240 min	[58]
21.	ZnO	MOF derived porus ZnO/C Nanocomposites	Methylene Blue	180 min	[59]
22.	ZnO	polymeric g-C_3N_4 composite	Methylene Blue	60 min	[60]
23.	ZnO	Activated Carbon	Methylene Blue	14 min	Present Work

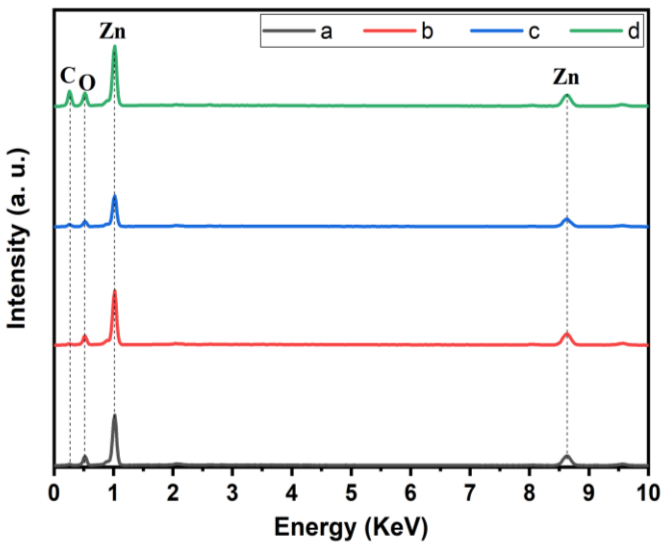

Fig. 4 Compositional Analysis of Annealed (a), (b), (c), (d).

Figure 6 shows the photodegradation of Eosin-Y 'a', 'b', 'c', and 'd'. Bare ZnO, *i.e.* (a) degrades in 70 min, ZnO /AC (2:1) *i.e.* (b) degrades in 70 min as the active sites available not much as compared to bare ZnO. In (c) the concentration of Activated carbon is equal to the ZnO, therefore, dye degrades in 35 min. In (d) the Activated carbon concentration is twice the bare ZnO which degrades in 18 min.

Figure 7 shows the photodegradation of Rose Bengal 'a', 'b', 'c', and 'd'. Bare ZnO, *i.e.* (a) degrades in 80 min, ZnO /AC (2:1), *i.e.* (b) degrades in 80 min as the active sites available not much as compared to bare ZnO. In (c) the concentration of Activated carbon is equal to the ZnO, therefore, dye degrades in 40 min. In (d) the Activated carbon concentration is twice the bare ZnO which degrades in 25 min. Table 2 shows the literature survey of composite material. Percentage degradation efficiency can be calculated using Beer-Lambert law, according to its concentration of dye is proportional to its absorbance shown in Equation (1).[61,62]

$$R = \frac{C_0 - C}{C_0} X\ 100 = \frac{A_0 - A}{A_0} X\ 100 \quad (1)$$

where C_0, A_0 is the concentration at an absorbance of dye at reaction condition time (0) and C, A is the concentration at an absorbance of dye at reaction condition time (t) minute respectively. the dye degradation percent efficiency has resulted in Table 3.

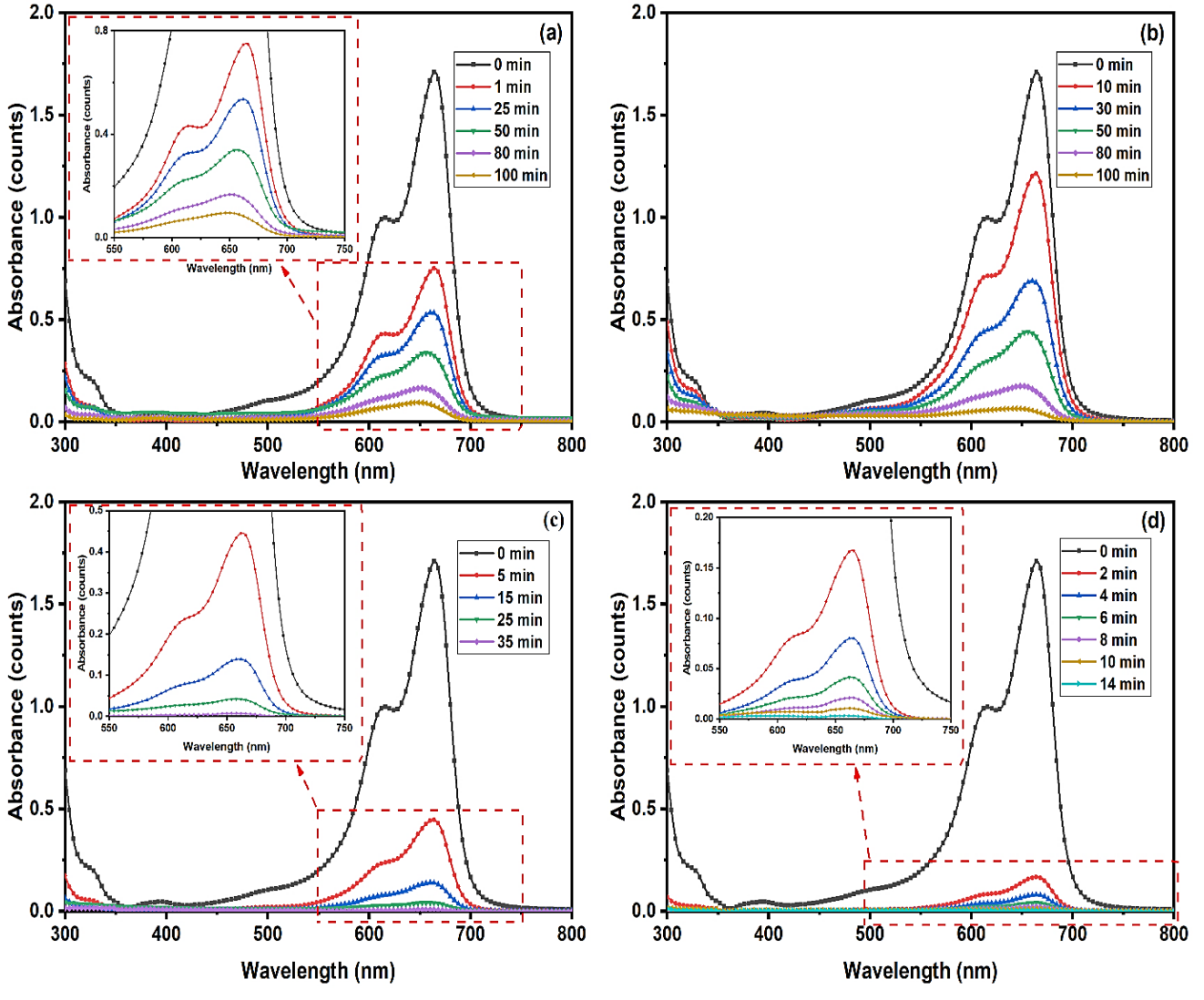

Fig. 5 Photodegradation of Methylene Blue Dye with ZnO Annealed (a), (b), (c), (d).

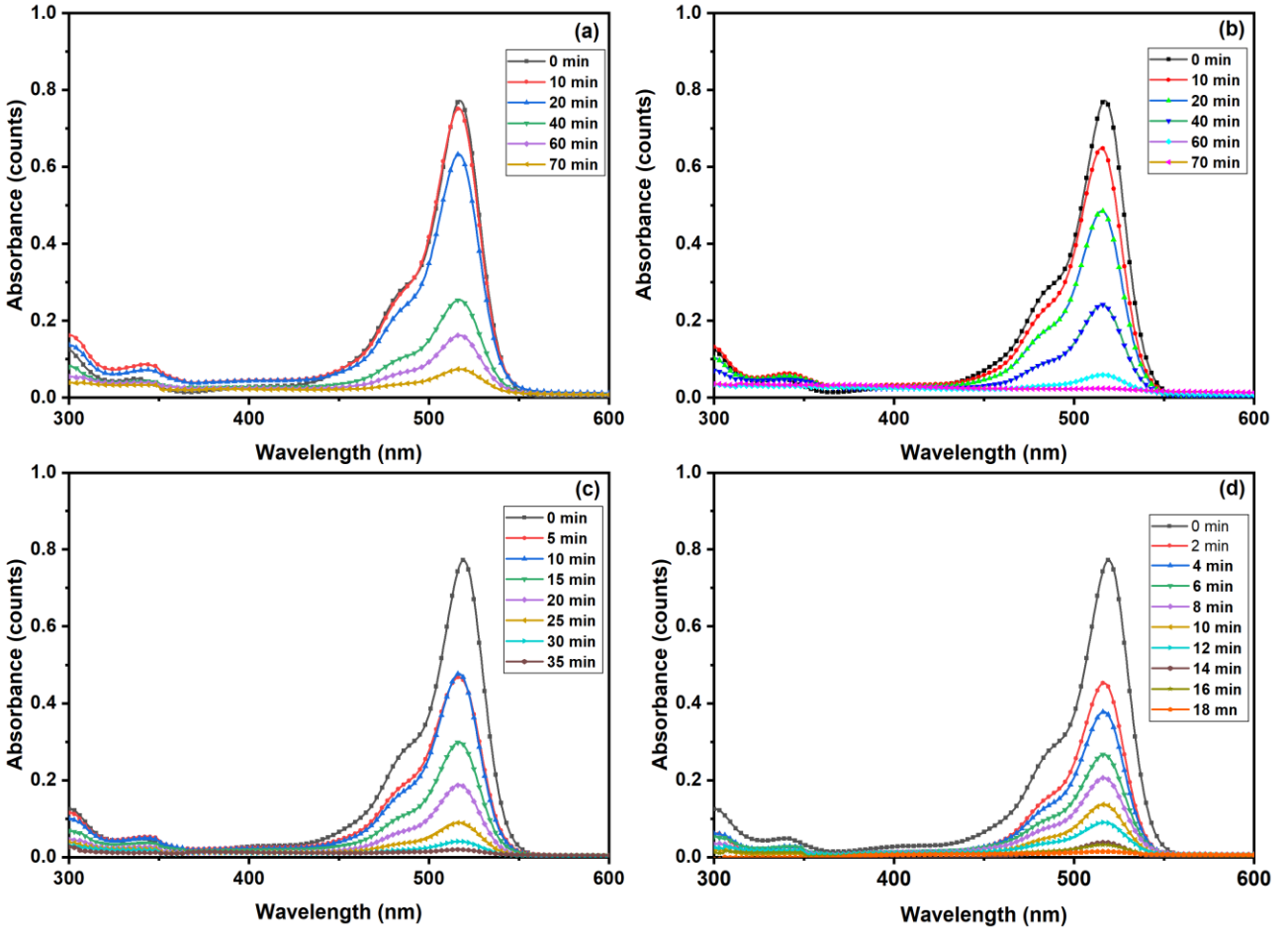

Fig. 6 Photodegradation of Eosin-Y with ZnO Annealed (a), (b), (c), (d).

The following Equation (2) shows kinetic model well explains the relation between the degradation of MB with the time of different samples.[63]

$$Rate = -\frac{dC}{dt} = \frac{kKC}{1+KC} \quad (2)$$

Where C is the concentration of dye (mg/L) at an instant t, t is the time for which the sample is irradiated, k is the first order constant of the reaction and K is the adsorption constant of dye on nanoparticles. Additionally, we can simplify this equation to pseudo-first-order-equation (3).[64]

$$\ln\left(\frac{C_t}{C_0}\right) = -kt \quad (3)$$

Furthermore, the half-life, $t_{1/2}$, can be calculated from the following Equation (4) and tabulated in Table 2.

$$t_{1/2} = \frac{\ln 2}{k} \quad (4)$$

Figure 8 shows Relative concentration versus irradiation time of (A) Methylene Blue (B) Eosin-Y (C) Rose Bengal for 'a', 'b', 'c', and 'd'. Figure 9 shows Plots of - ln (C/Co) versus irradiation time of of (A) Methylene Blue, (B) Eosin-Y, (C) Rose Bengal 'a', 'b', 'c', and 'd'. Figure 10 shows Plots of Photodegradation Efficiency versus irradiation time ZnO Annealed (a), (b), (c), (d).

3.6 Mechanism of photocatalytic reaction

The Kinetics of Methylene Blue Dye degradation can be explained as follows. When visible light is incident Activated Carbon and MG act as a photosensitizer and transfers the electron to the conduction band of ZnO. As the conduction band of ZnO has negative potential, they reduce O_2 to $\cdot O_{2-}$ superoxide. These superoxide radicals adsorb H_2O molecules on the surface of the catalyst and H^+ ions from the solution form hydroperoxyl.OH, radicals. The holes (h^+) in the valence band of ZnO/AC form OH^- radicals. The oxidized radical (OH) deeply oxidizes MB to form degraded products.

$$AC + h\upsilon = AC^*$$
$$AC^* + ZnO = (e_{CB}^-)\,ZnO + AC^{*+}$$
$$AC^{*+} = AC + h_{VB}^+$$
$$MB + h\upsilon = MB^*$$
$$MB^* + ZnO = (e_{CB}^-)ZnO + MB^{*+}$$
$$MB^{*+} = MB + h_{VB}^+$$
$$ZnO/\mathrm{AC} + h\upsilon = (e_{CB}^-)\mathrm{ZnO/AC} + h_{VB}^+\ \mathrm{ZnO/AC}$$
$$e_{CB\ in\ ZnO}^- + O_2 = \mathrm{ZnO} + \cdot O_2^-$$
$$\cdot O_2 + \mathrm{H2O} = \cdot \mathrm{HO} + OH^-$$
$$\cdot O_2^- + H^+ = \cdot OH_2$$
$$2 \cdot HO_2 = H_2O_2 + O_2$$
$$H_2O_2 + e^- = \cdot OH + OH^-$$
$$h_{VB\ in\ ZnO}^+ + OH^- = ZnO/\mathrm{AC} + \cdot \mathrm{OH}$$
$$\cdot OH + MB = degradation\ products$$
$$\frac{ZnO}{\mathrm{AC}(h_{VB}^+)(\mathrm{direct\ holes})} + MB = degradation\ products$$

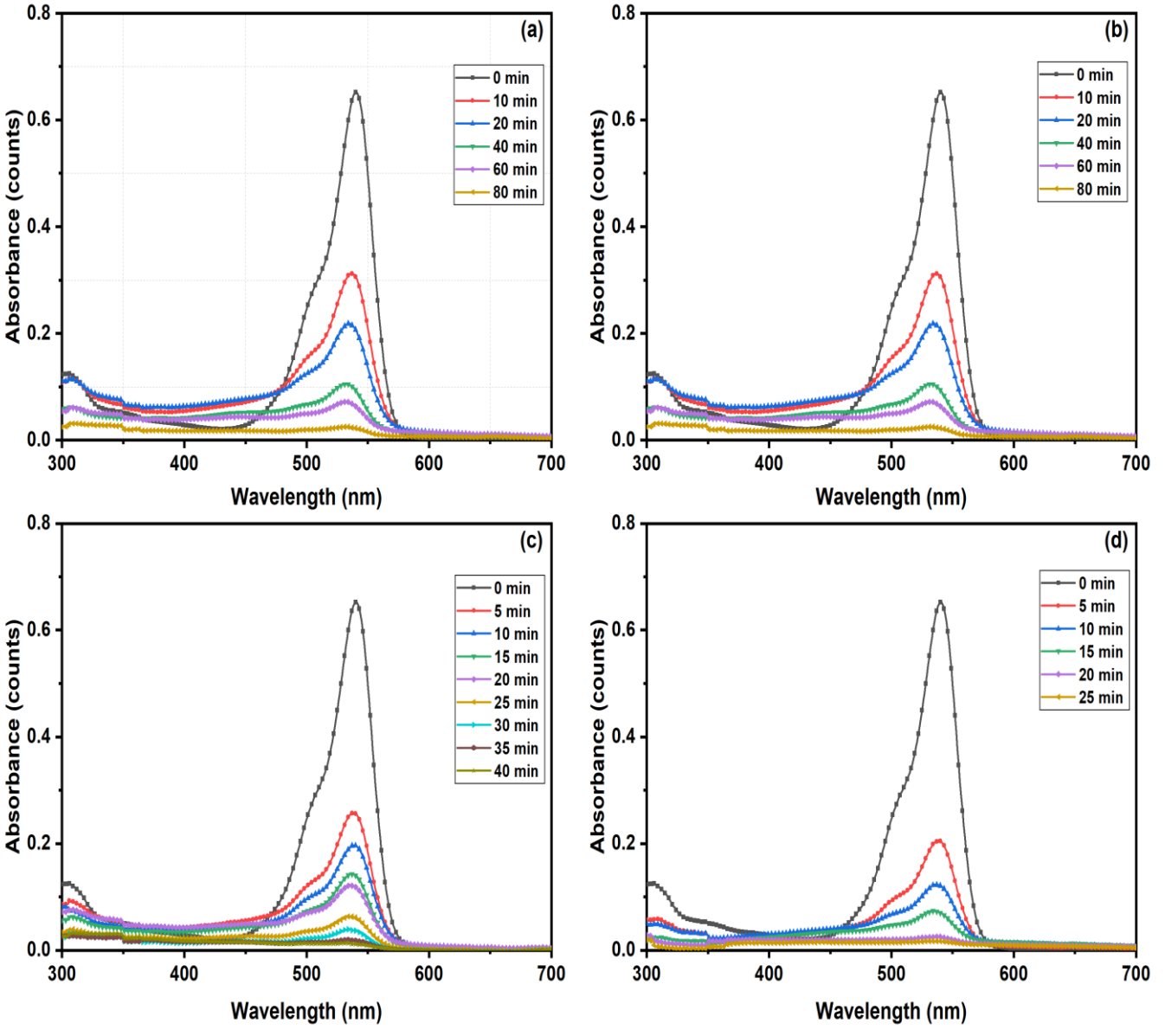

Fig. 7 Photodegradation of Rose Bengal with ZnO Annealed (a), (b), (c), (d).

Table 3. Rate Constant and Half-Life of of Annealed of (a), (b), (c), (d).

Sample	(a)		
Dye	Methylene Blue	Eosin-Y	Rose Bengal
Rate constant(k) (mm^{-1})	0.16	0.02	0.04
Half-life (min)	4.32	32.8	15.69
Sample	(b)		
Dye	Methylene Blue	Eosin-Y	Rose Bengal
Rate constant(k) (mm^{-1})	0.02	0.04	0.04
Half-life (min)	25.95	14.51	14.24
Sample	(c)		
Dye	Methylene Blue	Eosin-Y	Rose Bengal
Rate constant(k) (mm^{-1})	0.15	0.07	0.09
Half-life (min)	4.47	9.56	7.02
Sample	(d)		
Dye	Methylene Blue	Eosin-Y	Rose Bengal
Rate constant(k) (mm^{-1})	0.57	0.17	0.14
Half-life (min)	1.19	3.85	4.85

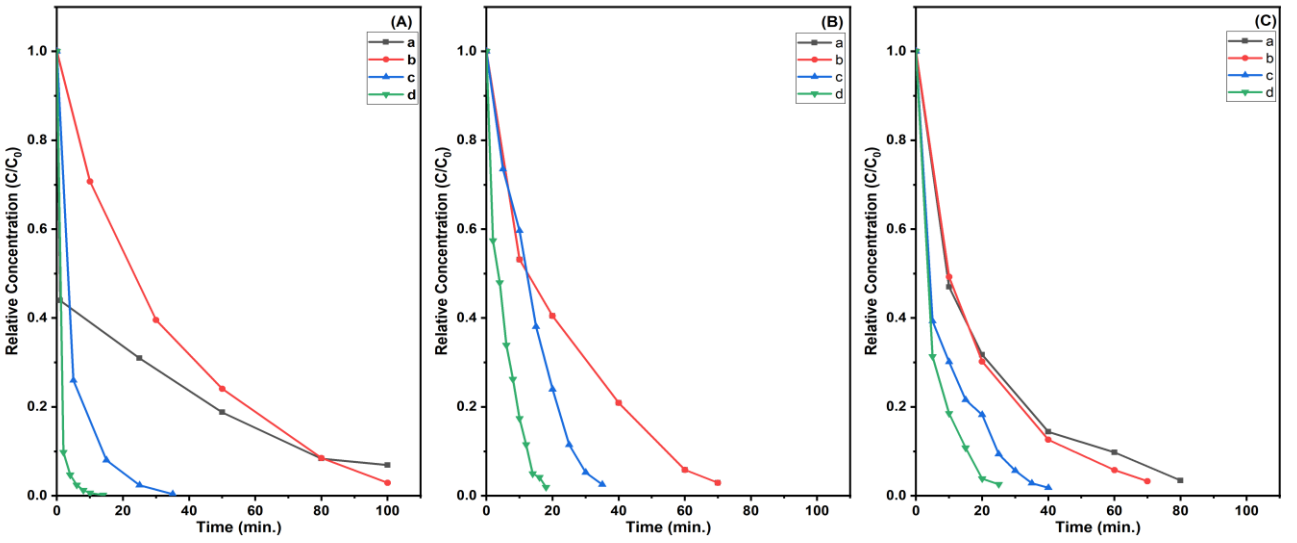

Fig. 8 Relative concentration versus irradiation time of ZnO Annealed (a), (b), (c), (d).

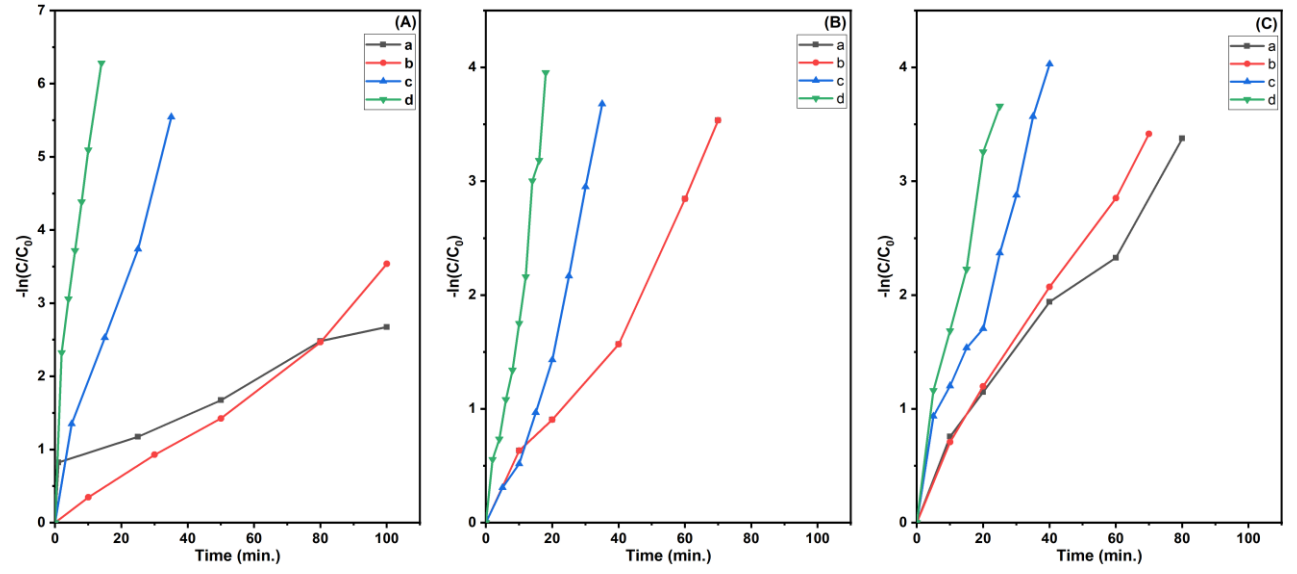

Fig. 9 Plots of - ln (C/Co) versus irradiation time of ZnO Annealed (a), (b), (c), (d).

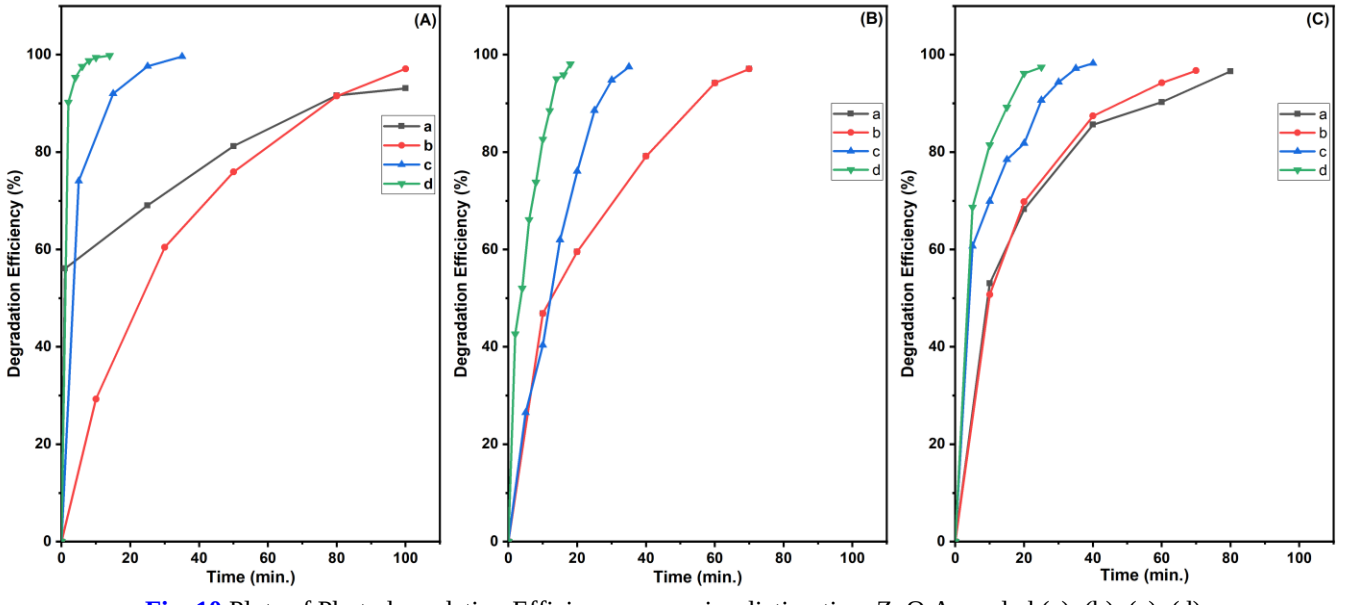

Fig. 10 Plots of Photodegradation Efficiency versus irradiation time ZnO Annealed (a), (b), (c), (d).

4. Conclusion

In this work, ZnO/AC for various ratios of the composite was synthesized using the reflux method. XRD, UV-visible, and SEM analysis reveal the composite of AC into ZnO. The XRD showed a wurtzite structure. The UV-Visible spectra showed a 3.2 eV band gap. The photovoltaic activity of methylene blue was found to be higher under visible light irradiation with activated carbon composite with ZnO was found to be in 14 min. With the increase in irradiation time the photodegradation efficiency increases. So, ZnO composite with AC is found to be effective to treat contaminated water from various textile industries.

Acknowledgement

CVJ is grateful to the Kiran Division, Department of Science and Technology, Government of India, for partial financial support through Women Scientist Scheme-A, vide Sanction Order SR/WOS-A/PM-11/2019(G).

Conflict of Interest

There is no conflict of interest.

Supporting Information

Not applicable.

References

[1] R. B. Rajput, S. N. Jamble, R. B. Kale, Solvothermal synthesis of anatase TiO_2 for the detoxification of methyl orange dye with improved photodegradation efficiency, *Engineered Science*, 2021, **17**, 176-184, doi: 10.30919/es8d534.

[2] M. S. Nasrollahzadeh, M. Hadavifar, S. S. Ghasemi, M. Arab Chamjangali, Synthesis of ZnO nanostructure using activated carbon for photocatalytic degradation of methyl orange from aqueous solutions, *Applied Water Science*, 2018, **8**, 1-12, doi: 10.1007/s13201-018-0750-6.

[3] E. Routoula, S. V. Patwardhan, Degradation of anthraquinone dyes from effluents: a review focusing on enzymatic dye degradation with industrial potential, *Environmental Science & Technology*, 2020, **54**, 647-664, doi: 10.1021/acs.est.9b03737.

[4] V. Katheresan, J. Kansedo, S. Y. Lau, Efficiency of various recent wastewater dye removal methods: a review, *Journal of Environmental Chemical Engineering*, 2018, **6**, 4676-4697, doi: 10.1016/j.jece.2018.06.060.

[5] R. Kumar, A. Umar, R. Kumar, M. S. Chauhan, G. Kumar, S. Chauhan, Spindle-like Co_3O_4-ZnO nanocomposites scaffold for hydrazine sensing and photocatalytic degradation of rhodamine B dye, *Engineered Science*, 2021, **16**, 288-300, doi: 10.30919/es8d548.

[6] D. R. Shinde, I. S. Quraishi, R. A. Pawar, An efficient visible light driven photocatalytic removal of dyes from the dye effluent using metal halide lamp based slurry reactor, *ES Energy & Environment*, 2021, **14**, 54-62, doi: 10.30919/esee8c504.

[7] P. Birnal, M. C. Marco de Lucas, I. Pochard, F. Herbst, O. Heintz, L. Saviot, B. Domenichini, L. Imhoff, Visible-light photocatalytic degradation of dyes by TiO_2-Au inverse opal films synthesized by Atomic Layer Deposition, *Applied Surface Science*, 2023, **609**, 155213, doi: 10.1016/j.apsusc.2022.155213.

[8] S. Bhowmick, C. P. Saini, B. Santra, L. Walczak, A. Semisalova, M. Gupta, A. Kanjilal, Modulation of the work function of TiO_2 nanotubes by nitrogen doping: implications for the photocatalytic degradation of dyes, *ACS Applied Nano Materials*, 2023, **6**, 50-60, doi: 10.1021/acsanm.2c03587.

[9] S. A. Kumar, M. Jarvin, S. Sharma, A. Umar, S. S. R. Inbanathan, N. P. Lalla, Facile and green synthesis of MgO nanoparticles for the degradation of victoria blue dye under UV irradiation and their antibacterial activity, *ES Food & Agroforestry*, 2021, **5**, 14-19, doi: 10.30919/esfaf519.

[10] Fuad, Ameen, Ecofriendly and low-cost synthesis of ZnO nanoparticles from *Acremonium potronii* for the photocatalytic degradation of azo dyes, *Environmental Research*, 2021, **202**, 111700, doi: 10.1016/j.envres.2021.111700.

[11] Weilai, Yu, New insight into the enhanced photocatalytic activity of N-, C- and S-doped ZnO photocatalysts, *Applied Catalysis B: Environmental*, 2016, **181**, 220-227, doi: 10.1016/j.apcatb.2015.07.031.

[12] T.-K. Hong, N. Tripathy, H.-J. Son, K.-T. Ha, H.-S. Jeong, Y.-B. Hahn, A comprehensive *in vitro* and *in vivo* study of ZnO nanoparticles toxicity, *Journal of Materials Chemistry B*, 2013, **1**, 2985, doi: 10.1039/c3tb20251h.

[13] S. Chaudhary, A. Umar, K. Bhasin, S. Baskoutas, Chemical sensing applications of ZnO nanomaterials, *Materials*, 2018, **11**, 287, doi: 10.3390/ma11020287.

[14] A. Djurišić, Y. H. Leung, Optical properties of ZnO nanostructures, *Small*, 2006, **2**, 944-961, doi: 10.1002/smll.200600134.

[15] Y. Liao, Y. Wang, L. Ouyang, Y. Dong, J. Zhou, Q. Hu, B. Qiu, Conductive polyaniline enhanced decolorization of azo dyes in anaerobic wastewater treatment, *ES Food & Agroforestry*, 2021, **6**, 35-42, doi: 10.30919/esfaf584.

[16] S. Sakthivel, B. Neppolian, M. V. Shankar, B. Arabindoo, M. Palanichamy, V. Murugesan, Solar photocatalytic degradation of azo dye: comparison of photocatalytic efficiency of ZnO and TiO_2, *Solar Energy Materials and Solar Cells*, 2003, **77**, 65-82, doi: 10.1016/s0927-0248(02)00255-6.

[17] B. Liu, H. C. Zeng, Hydrothermal synthesis of ZnO nanorods in the diameter regime of 50 nm, *Journal of the American Chemical Society*, 2003, **125**, 4430-4431, doi: 10.1021/ja0299452.

[18] L. Znaidi, Sol-gel-deposited ZnO thin films: a review, *Materials Science and Engineering: B*, 2010, **174**, 18-30, doi: 10.1016/j.mseb.2010.07.001.

[19] H. Ghorbani, F. Mehr, H. Pazoki, B. Rahmani, Synthesis of ZnO nanoparticles by precipitation method, *Oriental Journal of Chemistry*, 2015, **31**, 1219-1221, doi: 10.13005/ojc/310281.

[20] B. Woei, Chieng, Synthesis of ZnO nanoparticles by modified polyol method, *Materials Letters*, 2012, **73**, 78-82, doi: 10.1016/j.matlet.2012.01.004.

[21] X. Bai, L. Li, H. Liu, L. Tan, T. Liu, X. Meng, Solvothermal synthesis of ZnO nanoparticles and anti-infection application *in vivo*, *ACS Applied Materials & Interfaces*, 2015, **7**, 1308-1317,

doi: 10.1021/am507532p.
[22] S. D. Lee, S.-H. Nam, M.-H. Kim, J.-H. Boo, Synthesis and photocatalytic property of ZnO nanoparticles prepared by spray-pyrolysis method, *Physics Procedia*, 2012, **32**, 320-326, doi: 10.1016/j.phpro.2012.03.563.
[23] M. Tokumoto, V. Briois, C. Santilli and S. Pulcinelli, Preparation of ZnO Nanoparticles: Structural Study of the Molecular Precursor, *Journal of Sol-Gel Science and Technology*, 2003, **26**, 547-551, doi: 10.1023/A:1020711702332
[24] D. Dey, Roy, Ultra-low voltage adenine based gas sensor to detect H_2 and NH_3 at room temperature: first-principles paradigm, *International Journal of Hydrogen Energy*, 2023, **48**, 4931-4941, doi: 10.1016/j.ijhydene.2022.11.040.
[25] M. Qi, Q. Hou, Y. Li, First principles study of the effect of (Mg, C) doping and Zn vacancies on the carrier activity, lifetime, visible light effect, and oxidation-reduction reaction of ZnO (001) monolayers, *Applied Surface Science*, 2023, **616**, 156477, doi: 10.1016/j.apsusc.2023.156477.
[26] Z.-Y. Zhang, H.-M. Xiong, Photoluminescent ZnO nanoparticles and their biological applications, *Materials*, 2015, **8**, 3101-3127, doi: 10.3390/ma8063101.
[27] A. Wibowo, M. A. Marsudi, M. I. Amal, M. B. Ananda, R. Stephanie, H. Ardy, L. J. Diguna, ZnO nanostructured materials for emerging solar cell applications, *RSC Advances*, 2020, **10**, 42838-42859, doi: 10.1039/d0ra07689a.
[28] Atiq, U. Rehman, Impact of ZnO on structural and electrochemical properties of silver spinel ferrites for asymmetric supercapacitors, *Journal of Electroanalytical Chemistry*, 2023, **931**, 117206, doi: 10.1016/j.jelechem.2023.117206.
[29] S. Sohrabnezhad, A. Seifi, The green synthesis of Ag/ZnO in montmorillonite with enhanced photocatalytic activity, *Applied Surface Science*, 2016, **386**, 33-40, doi: 10.1016/j.apsusc.2016.05.102.
[30] M. Ali Karimi, A. Hatefi-Mehrjardi, A. Askarpour Kabir, M. Zaydabadi, Synthesis, characterization, and application of MgO/ZnO nanocomposite supported on activated carbon for photocatalytic degradation of methylene blue, *Research on Chemical Intermediates*, 2015, **41**, 6157-6168, doi: 10.1007/s11164-014-1729-z.
[31] M. Godino-Ojer, S. Morales-Torres, E. Pérez-Mayoral, F. J. Maldonado-Hódar, Enhanced catalytic performance of ZnO/carbon materials in the green synthesis of poly-substituted quinolines, *Journal of Environmental Chemical Engineering*, 2022, **10**, 106879, doi: 10.1016/j.jece.2021.106879.
[32] Rusheng, Yuan, Surface characteristics and photocatalytic activity of TiO_2 loaded on activated carbon fibers, *Colloids and Surfaces A: Physicochemical and Engineering Aspects*, 2005, **254**, 131-136, doi: 10.1016/j.colsurfa.2004.11.027.
[33] V. H. Tran Thi, B. K. Lee, Great improvement on tetracycline removal using ZnO rod-activated carbon fiber composite prepared with a facile microwave method, *Journal of Hazardous Materials*, 2017, **324**, 329-339, doi: 10.1016/j.jhazmat.2016.10.066.
[34] C. V. Jagtap, V. S. Kadam, M. A. Mahadik, J. S. Jang, N. B. Chaure, H. M. Pathan, Effect of binder concentration and dye loading time on titania based photoanode in DSSC application, *Engineered Science*, 2021, **17**, 133-41, doi: 10.30919/es8d581.
[35] V. Kadam, C. Jagtap, T. Alshahrani, F. Khan, M. T. Khan, N. Ahmad, A. Al-Ahmed, H. Pathan, Influence of CdS sensitization on the photovoltaic performance of CdS: TiO_2 solar cell, *Journal of Materials Science: Materials in Electronics*, 2021, **32**, 28214-28222, doi: 10.1007/s10854-021-07198-2.
[36] A. Diacon, A. Mocanu, C. E. Răducanu, C. Busuioc, R. Șomoghi, B. Trică, A. Dinescu, E. Rusen, New carbon/ZnO/Li_2O nanocomposites with enhanced photocatalytic activity, *Scientific Reports*, 2019, **9**, 16840, doi: 10.1038/s41598-019-53335-7.
[37] E. Emil, G. Alkan, S. Gurmen, R. Rudolf, D. Jenko, B. Friedrich, Tuning the morphology of ZnO nanostructures with the ultrasonic spray pyrolysis process, *Metals*, 2018, **8**, 569, doi: 10.3390/met8080569.
[38] M. S. Yadav, N. Singh, A. Kumar, Synthesis and characterization of zinc oxide nanoparticles and activated charcoal based nanocomposite for supercapacitor electrode application, *Journal of Materials Science: Materials in Electronics*, 2018, **29**, 6853-6869, doi: 10.1007/s10854-018-8672-5.
[39] Q. Zhu, N. Liu, N. Zhang, Y. Song, M. S. Stanislaus, C. Zhao, Y. Yang, Mesoporous Fe_3O_4@Ag@TiO_2 nanocomposite particles for magnetically recyclable photocatalysis and bactericide, *Advanced Powder Technology*, 2018, **29**, 664-671, doi: 10.1016/j.apt.2017.12.008.
[40] Q. Zhu, N. Liu, N. Zhang, Y. Song, M. S. Stanislaus, C. Zhao, Y. Yang, Efficient photocatalytic removal of RhB, MO and MB dyes by optimized Ni/NiO/TiO_2 composite thin films under solar light irradiation, *Journal of Environmental Chemical Engineering*, 2018, **6**, 2724-2732, doi: 10.1016/j.jece.2018.04.017.
[41] Z. Feng, X. Lv, T. Wang, TiO_2 porous ceramic/Ag-AgCl composite for enhanced photocatalytic degradation of dyes under visible light irradiation, *Journal of Porous Materials*, 2018, **25**, 189-198, doi: 10.1007/s10934-017-0432-z.
[42] R. Liu, Z. Ji, J. Wang, J. Zhang, Mesocrystalline TiO_2/sepiolite composites for the effective degradation of methyl orange and methylene blue, *Frontiers of Materials Science*, 2018, **12**, 292-303, doi: 10.1007/s11706-018-0429-9.
[43] Renae, Hickman, TiO_2-PDMS composite sponge for adsorption and solar mediated photodegradation of dye pollutants, *Journal of Water Process Engineering*, 2018, **24**, 74-82, doi: 10.1016/j.jwpe.2018.05.015.
[44] A. Mishra, A. Mehta, S. Kainth, S. Basu, Effect of g-C_3N_4 loading on TiO_2/Bentonite nanocomposites for efficient heterogeneous photocatalytic degradation of industrial dye under visible light, *Journal of Alloys and Compounds*, 2018, **764**, 406-415, doi: 10.1016/j.jallcom.2018.06.089.
[45] B. Zhang, M. Li, X. Wang, Y. Zhao, H. Wang, H. Song, Pompon-like structured g-C_3N_4/ZnO composites and their application in visible light photocatalysis, *Research on Chemical Intermediates*, 2018, **44**, 6895-6906, doi: 10.1007/s11164-018-3528-4.
[46] L. Dong, W. Zhang, B. Sang, X. Li, D. Liu, ZnO/graphene nanomaterials construct by simple ultrasound method with increased photocatalytic performance, *Journal of Ovonic Research*, 2018, **14**, 475-782.
[47] G. J. F. Cruz, M. M. Gómez, J. L. Solis, J. Rimaycuna, R. L. Solis, J. F. Cruz, B. Rathnayake, R. L. Keiski, Composites of ZnO nanoparticles and biomass based activated carbon: adsorption, photocatalytic and antibacterial capacities, *Water Science and Technology*, 2018, **2017**, 492-508, doi: 10.2166/wst.2018.176.
[48] H. Xiao, W. Zhang, Y. Wei, L. Chen, Carbon/ZnO nanorods composites templated by TEMPO-oxidized cellulose and

photocatalytic activity for dye degradation, *Cellulose*, 2018, **25**, 1809-1819, doi: 10.1007/s10570-018-1651-4.
[49] H. Moussa, B. Chouchene, T. Gries, L. Balan, K. Mozet, G. Medjahdi, R. Schneider, Growth of ZnO nanorods on graphitic carbon nitride gCN sheets for the preparation of photocatalysts with high visible-light activity, *ChemCatChem*, 2018, **10**, 4973-4983, doi: 10.1002/cctc.201801206.
[50] A. Khan, J. C. Colmenares, R. Gläser, Lignin-based composite materials for photocatalysis and photovoltaics. Topics in Current Chemistry Collections. Cham: Springer International Publishing, 2018: 1-31, doi: 10.1007/978-3-030-00590-0_1.
[51] V. Gilja, I. Vrban, V. Mandić, M. Žic, Z. Hrnjak-Murgić, Preparation of a PANI/ZnO composite for efficient photocatalytic degradation of acid blue, *Polymers*, 2018, **10**, 940, doi: 10.3390/polym10090940.
[52] Pengfei, Hu, Efficient visible-light photocatalysis of ZIF-derived mesoporous $ZnFe_2O_4$/ZnO nanocomposite prepared by a two-step calcination method, *Materials Science in Semiconductor Processing*, 2018, **77**, 40-49, doi: 10.1016/j.mssp.2018.01.012.
[53] S. Ata, I. Shaheen, Qurat-ul-Ayne, S. Ghafoor, M. Sultan, F. Majid, I. Bibi, M. Iqbal, Graphene and silver decorated ZnO composite synthesis, characterization and photocatalytic activity evaluation, *Diamond and Related Materials*, 2018, **90**, 26-31, doi: 10.1016/j.diamond.2018.09.015.
[54] X. Hu, S. Han, Y. Zhu, Facet-controlled synthesis of polyhedral hematite/carbon composites with enhanced photoactivity, *Applied Surface Science*, 2018, **443**, 227-235, doi: 10.1016/j.apsusc.2018.02.266.
[55] Q. Shi, S. Wang, H. Wu, M. Yu, X. Su, F. Ma, J. Jiang, Synthesis and characterizations of V_2O_5/ZnO nanocomposites and enhanced photocatalytic activity, *Ferroelectrics*, 2018, **523**, 74-81, doi: 10.1080/00150193.2018.1391563.
[56] N. M. Denisov, E. B. Chubenko, V. P. Bondarenko, V. E. Borisenko, Black ZnO/C nanocomposite photocatalytic films formed by one-step Sol-gel technique, *Journal of Sol-Gel Science and Technology*, 2018, **85**, 413-420, doi: 10.1007/s10971-017-4554-1.
[57] D. Aljuboury, P. Palaniandy, Inorganic carbon removal from refinery wastewater by using TiO_2 /ZnO/fenton photocatalyst, *Global Nest Journal*, 2018, **20**, 216–25, doi: 10.30955/gnj.002374.
[58] M. M. Sabzehmeidani, H. Karimi, M. Ghaedi, Electrospinning preparation of NiO/ZnO composite nanofibers for photodegradation of binary mixture of rhodamine B and methylene blue in aqueous solution: central composite optimization, *Applied Organometallic Chemistry*, 2018, **32**, e4335, doi: 10.1002/aoc.4335.
[59] M. Z. Hussain, A. Schneemann, R. A. Fischer, Y. Zhu, Y. Xia, MOF derived porous ZnO/C nanocomposites for efficient dye photodegradation, *ACS Applied Energy Materials*, 2018, **1**, 4695-4707, doi: 10.1021/acsaem.8b00822.
[60] P. Murugesan, N. Girichandran, S. Narayanan, M. Manickam, Structural, optical and photocatalytic properties of visible light driven zinc oxide hybridized two-dimensional π-conjugated polymeric g-C_3N_4 composite, *Optical Materials*, 2018, **75**, 431-441, doi: 10.1016/j.optmat.2017.10.051.
[61] K. Wang, L. Yu, S. Yin, H. Li, H. Li, Photocatalytic degradation of methylene blue on magnetically separable FePc/Fe_3O_4 nanocomposite under visible irradiation, *Pure and Applied Chemistry*, 2009, **81**, 2327-2335, doi: 10.1351/pac-con-08-11-23.
[62] Y. Abdollahi, A. H. Abdullah, Z. Zainal, N. A. Yusof, Photocatalytic degradation of p-cresol by zinc oxide under UV irradiation, *International Journal of Molecular Sciences*, 2011, **13**, 302-315, doi: 10.3390/ijms13010302.
[63] X. Xu, R. Lu, X. Zhao, S. Xu, X. Lei, F. Zhang, D. G. Evans, Fabrication and photocatalytic performance of a $Zn_xCd_{1-x}S$ solid solution prepared by sulfuration of a single layered double hydroxide precursor, *Applied Catalysis B: Environmental*, 2011, **102**, 147-156, doi: 10.1016/j.apcatb.2010.11.036.
[64] A. Wood, M. Giersig, P. Mulvaney, Fermi level equilibration in quantum dot–metal nanojunctions, *The Journal of Physical Chemistry B*, 2001, **105**, 8810-8815, doi: 10.1021/jp011576t.